Polymersome production on a microfluidic platform using pH sensitive block copolymers

Luke Brown,[ab] Sally L. McArthur,[c] Phillip C. Wright,[a] Andrew Lewis[d] and Giuseppe Battaglia*[b]

Received 9th March 2010, Accepted 28th April 2010
DOI: 10.1039/c004036c

Development of pH sensitive biocompatible block copolymer polymersomes, which are stable in physiological conditions, is enabling the intracellular delivery of water soluble drugs and proteins. As a result, it is becoming increasingly important to develop robust production methods to enhance the polymersome encapsulation efficiency. One way that this could be achieved is through production in microfluidic devices that potentially offer more favourable conditions for encapsulation. Here a flow focussing microfluidic device is used to induce self-assembly of poly(2-(methacryloyloxy)ethyl phosphorylcholine)–poly(2-(diisopropylamino)ethyl methacrylate) (PMPC-*b*-PDPA) block copolymer by changing the pH of the flows within the microchannels. The laminar flow conditions within the device result in a pH gradient at either interface of the central flow, where diffusion of hydrogen ions enables the deprotonation of the PDPA block copolymer and results in self-assembly of polymersomes. Dynamic light scattering reveals hydrodynamic diameters in the range of 75–275 nm and double membrane structures visualized using transmission electron microscopy indicate that polymersome nanostructures are being produced. The encapsulation efficiency for Bovine Serum Albumin (BSA) was calculated by measuring the spectroscopic absorbance at 279 nm and indicates that the encapsulation efficiency produced in the microfluidic device is equivalent to the standard in solution production method. Critically, the microfluidic system eliminates the use of organic solvents, which limit biological applications, through the pH induced self-assembly process and offers a continuous production method for intracellular delivery polymersomes.

Introduction

The emergence of microfluidics has been driven by the great economy of scale that is offered when working with nanolitre volumes within these devices as decreased throughput times, high surface to volume ratios and shorter diffusion distances not only result in faster reaction times, but also at a reduced cost.[1,2] There are a number of advantages offered by microfluidics, especially the continuous reproducible nature of laminar flow with low Reynolds numbers ordinarily seen at this length scale.[3] This has resulted in their use in particle production applications with the development of a large number of different microfluidic geometries including T-junction,[4] co-flowing,[5] glass capillary[6] and flow focussing.[7] Of these continuous devices a number are involved in the formation, synthesis and self-assembly of nanometre- and/or micrometre-sized particles including double emulsions, liposomes and polymersomes.[8,9] In particular, there is interest in developing techniques to control polymersome or liposome size and size distribution due to their importance to act as encapsulates for various agents. Traditional production methods suffer from high polydispersities, offer poor encapsulation efficiencies and often require additional post-processing steps.[9,10] Microfluidic systems are seen as a way of providing the high level of control over chemical synthesis and self-assembly required, that exists in the cellular environment where nanoparticles such as polymersomes are reproducibly produced in a locally controlled environment.[11]

Device developments are being seen for block copolymer polymersomes, which are the synthetic version of liposomes and are currently being used to encapsulate DNA,[12] drugs,[13] and contrast agents[14] with subsequent delivery into cells. There is particular interest in the development of microfluidic systems that can provide alternative drug delivery methods and enable the specific targeted delivery of specialized drugs.[15] Advancements toward this high level of control over properties are occurring with the formation of hydrogel particles,[16] specifically that of calcium alginate beads,[2,17] polymersome formation *via* solvent evaporation from double emulsions templates[18,19] and polymeric microcapsule formation through UV photopolymerization.[20] There are also good examples of the self-assembled structures currently being developed within the field of synthetic biology to fabricate constructs that are analogous to natural systems.[21] Here the superior polymersome properties make them ideal biomimetic nanoscale reaction containers and enable them to be developed for these bottom up construction processes.[22]

Block copolymers have an amphiphilic nature that enables them to form a range of structures. The conformation of the structures is governed by polymer molecular weight, the volume fraction of each block and the interaction energy between monomer blocks.[23] All of the structures arise from the

[a]*ChELSI Institute, Department of Chemical and Process Engineering, University of Sheffield, UK*
[b]*Department of Biomedical Sciences, University of Sheffield, UK. E-mail: G.Battaglia@sheffield.ac.uk*
[c]*IRIS Faculty of Engineering and Industrial Science, Swinburne University of Technology, Australia*
[d]*Biocompatibles Ltd, Farnham, UK*

amphiphilic nature of the copolymer blocks. Self-assembly results from the hydrophobic effect causing the hydrophobic chains to minimise their interactions with water, and hydration forces that enable the hydrophilic chains to interact with the solvent.[24] Polymersomes are formed at low concentrations in water where the amphiphiles are dispersed into isotropic supramolecular structures.[25] These polymersomes offer superior mechanical properties to lipid vesicles due to the conformational freedom and increased length of the polymer chains, but more importantly the wide range of block copolymer chemistries available will enable application specific novel membranes to be developed.[26] One chemistry that has been developed uses poly(2-(methacryloyloxy)ethyl phosphorylcholine)–poly-(2-(diisopropylamino)ethyl methacrylate) (PMPC-*b*-PDPA) block copolymers to induce polymersome formation *via* changes in pH. The PDPA polymer chain is completely dissolved in water below pH 6, but becomes insoluble above this pH due to deprotonation of its tertiary amine groups. Thus above pH 6 the block copolymer self-assembles to form polymersomes.[27] These polymersomes are stable in physiological conditions and are being used for intracellular delivery of encapsulated DNA and proteins.[12,28,29]

The formation processes for polymersomes typically involve film rehydration[30] or electroformation.[31] However, these are bulk production methods which require post-processing steps, such as extrusion and sonication, due to the large polydispersity of the polymersomes produced and they also have an inherent encapsulation efficiency limit.[32] This is potentially a very restrictive factor in terms of the levels of expensive encapsulates that are lost, but also due to the difficulties in quantifying the dose contained within a certain volume of polymersomes. Attempts to solve these problems have led to the development of microfluidic methods for producing block copolymer polymersomes using devices based on glass microcapillary geometries, which produce giant polymersomes in the micron sized range.[18] These devices produce double emulsions comprising water within organic solvent droplets, which contain the block copolymers, in a water environment. The polymersomes are formed by evaporating the solvent to leave the diblock copolymer membrane containing an aqueous droplet that will contain any hydrophilic encapsulates.[18,33] This double emulsion method has been used with biocompatible and biodegradable block copolymers to encapsulate small hydrophilic solutes with high efficiency levels.[34] However, the extent of retention of solvent within the membrane structure after evaporation is unknown and may render the polymersomes unsuitable for biological and pharmaceutical applications.[18] The assembly of pH sensitive block copolymers within microfluidic devices eliminates the use of solvents creating a new route for bioactive polymersome production.

Thus, this current work introduces a new continuous method for producing block copolymer polymersomes using pH changes within a flow focussing microfluidic device, which significantly negates the use of organic solvents. It is possible to optimise the conditions within the device in a controlled manner to enable the pH switch of PMPC-*b*-PDPA to occur and result in the formation of polymersomes. The changes in pH of the flow, the polydispersity and the encapsulation efficiency of the device are calculated in order to determine how effective the microfluidic platform is for the continuous production of polymersomes.

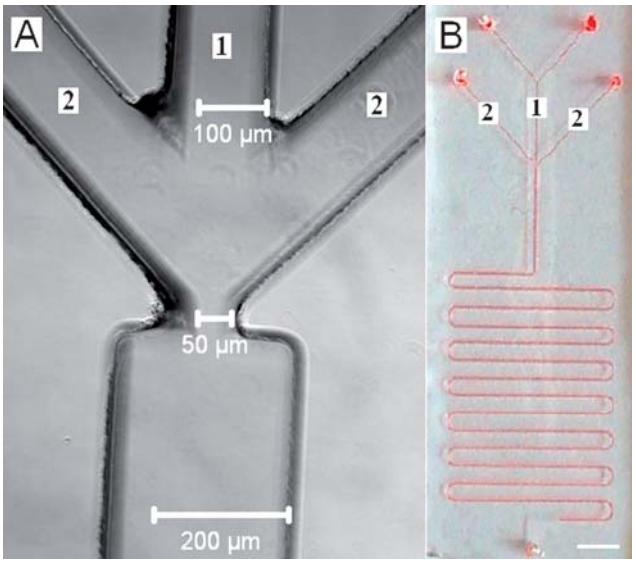

Fig. 1 (A) A light microscope image focused on the narrow orifice where the three flows meet in the flow focussing microfluidic device. (B) A photograph of an entire oxygen sealed device where the channels have been highlighted using food dye. In both images, the 1's indicate a flow of pH 6 polymer solution, which may also contain any molecules to be encapsulated, such as BSA, and the 2's represent aqueous flows of basic PBS buffers. Scale bar of B is 0.5 cm.

Materials and methods

(1) Microfluidic device manufacture

There are well established soft lithography techniques that have been developed for the production of polydimethylsiloxane (PDMS, Sylgard 184, Dow Corning) microfluidic devices using positive relief SU8 photoresist masters. This enables specific microchannel designs to be rapidly cast and then sealed irreversibly after all surfaces are treated in an oxygen plasma.[35–37] This current work uses these proven techniques to produce a basic flow focussing microfluidic device with a serpentine channel. A covalently sealed PDMS and glass device is shown in Fig. 1.

(2) Polymersome production

The basis for polymersome production using this microfluidic system is the pH sensitive block copolymer $PMPC_{25}$-*b*-$PDPA_{70}$ that is produced using Atom Transfer Radical Polymerisation (ATRP) as previously described.[38] The PDPA block has a $pK_a \approx 6.2$ enabling it to undergo deprotonation of its amine groups in basic solutions, becoming soluble. The block copolymer solutions were prepared, usually at 5 mg ml^{-1}, by dissolving the polymer in PBS solution (pH 2, 100 nM) before increasing the pH with 1 M NaOH. Once the polymer solution reached pH 6 it was passed through a 0.2 μm filter (Sarstedt) prior to use. The polymer solution is placed in a 1 ml glass syringe mounted on a syringe pump (Kent Scientific) to enable it to be flowed through the central channel of the device. Filtered aqueous PBS buffers at various values of pH are flowed through the outer two channels, labelled 2 in Fig. 1. Various flow rate ratios of the central to

external channels were used, ranging from 1 : 3 (16 : 48 μl min^{-1}) to 1 : 6 (8 : 48 μl min^{-1}), to induce the self-assembly of polymersomes.

(3) Polymersome characterisation

Visualisation of the flow within the microfluidic channel was carried out on an inverted confocal laser scanning microscope (Zeiss, LSM 510 META) using the pH indicator dextran, SNARF®-1, M_w 10 000 (Invitrogen). A series of images were taken using a multichannel set up with a 488 nm HeNe laser. The pH sensitive fluorophore was introduced through the central channel at pH 6. With excitation at 488 nm two separate channel settings were established to detect the changes in emission spectra produced with the variation in pH across the channels. This was initially performed using a single flow of calibration solutions at known pH values to produce a standard curve of pH *versus* intensity ratio of the 638 nm peak over the 590 nm peak, as identified *via* spectrophotometry. The curve was then used to establish the pH of the standard three flow system by sequentially analysing the intensity ratio of the two peaks for the images throughout the length of the device.

To determine the size of the polymeric nanostructures being formed Dynamic Light Scattering (DLS) was performed at 90° using a 633 nm HeNe laser (Brookhaven), along with Transmission Electron Microscopy (TEM) (FEI Tecnai G2 Spirit TEM). Finally, to determine the encapsulation efficiency of the device, the protein Bovine Serum Albumin (BSA) (Fluka) was dissolved in the polymer solution at pH 6 and flowed through the central channel. Upon collection approximately 230 μl of polymersome containing solution were passed through a sepharose (Sigma) extrusion column, to remove the excess protein. Fractions (~430 μl) of the filtered solution are collected sequentially to ensure only the polymersomes are retained. The absorbance of the samples is recorded using a UV-visible spectrophotometer (Jasco V-630) to ensure polymersomes are present and to enable the BSA absorbance peak at 279 nm to be measured. This information is used along with the known input solution data to determine the encapsulation efficiency for the device. This can then be compared to that of the standard in solution production method of polymersome formation.

Results and discussion

Developing conditions for polymersome formation

To produce block copolymer polymersomes using a microfluidic platform, it was first necessary to create the correct flow conditions within the device to induce formation through a controlled pH shift. The block copolymer $PMPC_{25}$-*b*-$PDPA_{70}$ remains in solution below pH 6.4 with nanostructures formed above this value. By introducing basic solutions within the correct pH range the local pH at the flow interfaces can be increased to cause the spontaneous self-assembly of polymersome nanostructures. Introducing the copolymer at pH 6 through the central channel of the device uses the inherent laminar flow conditions of flow focussing devices with miscible liquids to induce the shift in pH at the interface between the two solutions. The copolymer polymersomes should form at this interface as mixing occurs between the two flows *via* diffusion, creating a pH gradient that will enable the tertiary amine groups on the PDPA block to deprotonate causing it to become insoluble, which will result in formation of nanoparticles.[27] The laminar flow pattern created by flow focussing of three miscible flows has successfully been used by other groups to produce monodisperse liposomes by taking advantage of the reproducible chemical and mechanical conditions across the stream width.[10] Thus, the same principles can be applied to the block copolymer polymersome formation within the microchannels.

Previous studies have identified the ideal conditions for stable polymersome formation.[27,39] For the self-assembly process to occur within the microchannels and produce stable polymersomes it is necessary for the pH of the solution exiting the device to be above pH 7.2. To achieve these conditions, a range of flow rates were investigated for a number of basic PBS input solutions and the data recorded are illustrated in Fig. 2. As the PBS solution became more basic there were a larger proportion of proton donors at the laminar flow interfaces to enable the deprotonation of the PDPA block to occur. This means it is possible to induce self-assembly of the entire solubilised polymer in solution increasing rapidly, with the increase in the final solution above pH 7.2 indicating this effect. There is, however, an upper limit to this process whereby any basic solution above approximately pH 10.5 triggers precipitation of the polymer within the microchannels. The image within Fig. 2 illustrates this phenomenon as the deprotonation process occurs too rapidly with the copolymers unable to stay within solution and they precipitate onto the device walls. Although this behaviour is not desired, it does clearly indicate the polymersome formation process is occurring at the laminar flow interface where the basic PBS solutions flow alongside the pH 6 polymer solution.

As expected the larger flow rate ratios resulted in a greater proportion of basic PBS solution entering the system and resulted in an overall increase in the pH of the solution. It can be seen that the 1 : 6 flow rate ratio offers the largest range of solutions that raise the pH above the 7.2 threshold and so it was primarily used as the ideal flow set up, with flows of 8 μl min^{-1} and 48 μl min^{-1}.

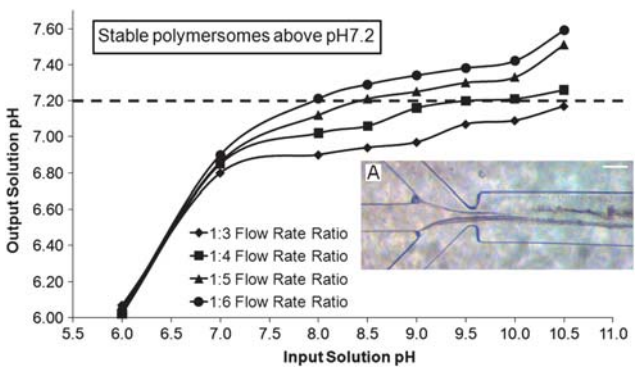

Fig. 2 Changes in the pH of the block copolymer solution for a number of different flow rate conditions using a range of basic PBS input solutions. The ratios refer to the flow rate of the polymer containing central channel at pH 6 to the two external channels at varying pH. (A) A light microscopy image of the polymer precipitation that occurs when using basic solutions of pH > 10.5.

Determining polymersome formation within the device

To clarify the laminar nature of the flow within the device, using the 1 : 6 flow rate ratio, and also to image the changes in pH that are occurring as the three flows interact, the fluorescent pH indicator SNARF was introduced through the central channel. The emission spectrum undergoes a pH dependent shift, with peaks at 590 nm and 638 nm varying in intensity. Subsequently, the confocal microscope was set up with two channels to collect the emission spectrum produced at these two wavelengths and images were recorded along the length of the device (see Fig. 3). The intensity of these two channels represents the changes in pH that are occurring, with an increase in intensity of the 638 nm channel reflecting an increase in the strength of the basic solution. From the images it is clear that the change in pH occurs gradually along the length of the device, through gentle diffusion at the flow interface, as the intensity of the 638 nm channel increases along the length of the microchannel. Additionally comparing the laminar flow image in Fig. 3B–D illustrates how this controlled diffusion of the hydrogen ions across the fluid interfaces results in a final solution of uniform pH. Fig. 3E illustrates an estimate of the pH of the central SNARF labelled flow throughout the length of the device as calculated from the ratio of the intensity of the two emission peaks. As expected, the pH increased rapidly up to the start of the serpentine channel due to the sudden influx of hydrogen ion acceptors introduced by the aqueous solutions. This rate decreases throughout the channel until a final uniform value is measured on exiting the device. These data indicate that it is possible for a microenvironment to be created within the device where a controlled change in the fluid conditions enables the self-assembly of the amphiphilic block copolymers into stable polymersome structures.

Having identified the correct conditions within the microchannels for the polymersomes to theoretically spontaneously form due to the shift in pH, the next step was to prove polymersome formation. To confirm self-assembly at the fluid interface a combination of DLS, to determine nanostructure size, and TEM, to clarify double membrane structure, was used. The results of the DLS analysis shown in Fig. 4 indicate that the structures are of a polymersome nature, with an effective hydrodynamic diameter of over 50 nm being consistent with other structures reported within the literature.[27] Both of the TEM images of double membrane nanostructures in the 100–200 nm range support the DLS data that the structures are polymersomes. The large variation in diameters seen within samples is a result of the lack of control that exists in the self-assembly process. This is typically seen in other bulk solution formation techniques, and a narrower polydispersity can be produced through downstream processing techniques such as extrusion and sonication.[40] Although the tighter polydispersity seen for the pH 9 input solution indicates that it may be possible to control the size distribution by controlling the rate of the pH induced self-assembly process. However, even if this is not attainable the drawback of a broad size distribution is no different to the standard production method, and again extrusion can be used to improve the polydispersity. However, the device offers the benefits of the continuous nature of the formation process providing reproducibility over the structures produced without the use of organic solvents. There is also the potential benefit of the ease at which downstream modifications to the channel geometries through soft lithography can be achieved, and there is the possibility of linking this system to a continuous pump extrusion system to automate the entire production process. Other techniques have been developed to improve the control over the size range, such as electroformation[30] and surface

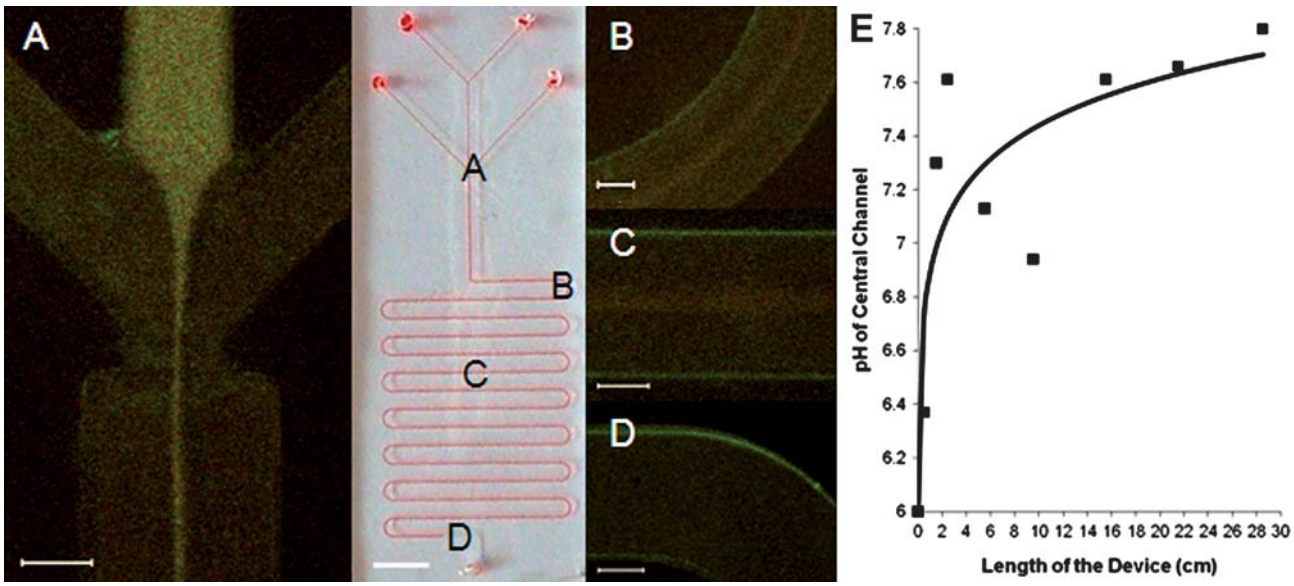

Fig. 3 Confocal images of the pH 6 flow through the central channel, containing the SNARF pH indicator, with pH 9 basic PBS solutions flowing either side in the standard 1 : 6 flow rate ratio, taken at various points in the device. (A) The flow focussing orifice, (B) ~2 cm travelled, (C) ~14 cm travelled and (D) ~26 cm travelled. The increase of the 638 nm channel intensity indicates an increase in the pH of the solution. The scale bars are 100 μm for images (A–D) and 0.5 cm for the device image. The graph in (E) illustrates the increase in pH that occurs throughout the length of the device as calculated from the ratio of the two SNARF peaks at 638 nm and 590 nm when compared to a standard curve of known intensities.

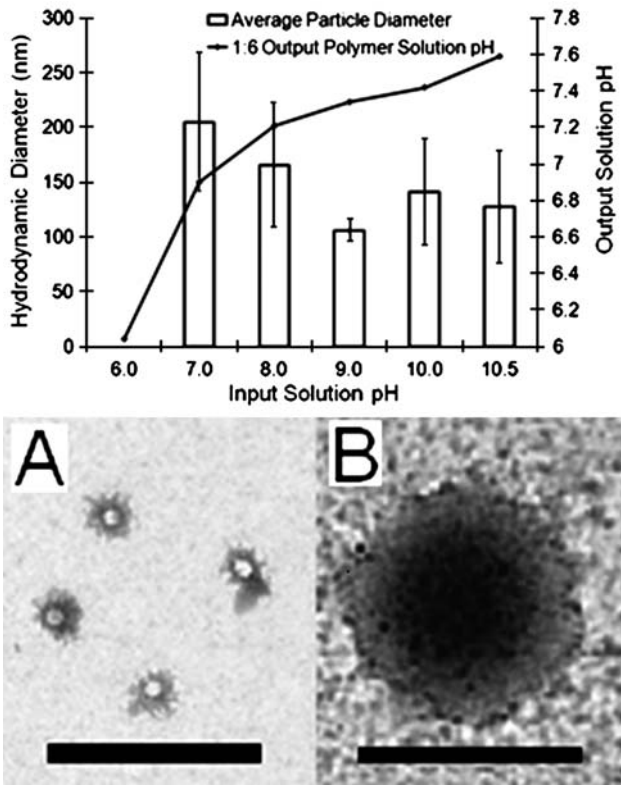

Fig. 4 The graph depicts changes in the hydrodynamic diameter, as measured by dynamic light scattering, and the resulting final solution pH that occurs with increasing the basicity of the PBS solution for the 1 : 6 flow rate ratio. (A and B) TEM images illustrating the structure of the polymersomes formed within the device, using a pH 10 buffer solution input. The scale bars are 1 μm and 0.2 μm respectively.

directed templating,[40] but as yet none can offer the benefits of continuous production.

Comparison of encapsulation efficiency

Polymersomes are the ideal transport vehicles into cells and as a result a great deal of work is centered around encapsulating molecules, such as DNA,[12,28,29] and contrast agents[14] inside these robust structures. So it is of critical importance that the formation process within the device enables the encapsulation of molecules on a par with the standard production methods. To test this efficiency, the protein BSA was chosen to be encapsulated and was dissolved in the polymer solution at pH 6. As it flows through the central channel the protein becomes encapsulated within the aqueous cores of the polymersomes as they undergo self-assembly. The efficiency of this process is calculated by measuring the BSA absorbance peak at 279 nm, using UV-visible spectrophotometry, of the protein encapsulated within the polymersomes and then comparing it to a BSA concentration curve. The same process was applied to polymersomes produced using the standard solution formation method. In this method, the polymersomes were formed by adding BSA to the polymer solution at pH 6, the solution was increased to pH 7.2, inducing self-assembly, before finally carrying out a 20 minute sonication to enhance encapsulation. Using the peak

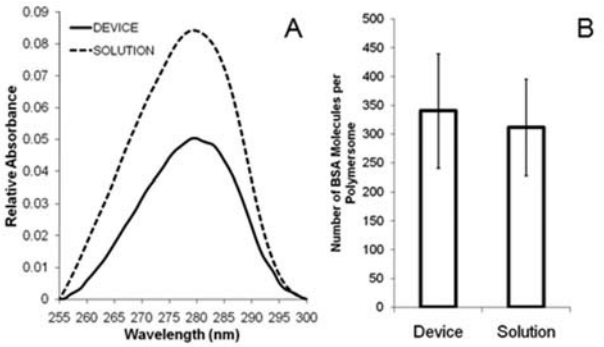

Fig. 5 Encapsulation of Bovine Serum Albumin analysis. (A) The average absorbance peaks at 279 nm as measured by UV-vis spectrophotometry where the BSA concentrations for the device and solution are approximately 1.2 mg ml^{-1} and 1.6 mg ml^{-1} respectively. (B) The average number of protein molecules encapsulated within the polymersomes for the two production processes.

adsorption values shown in Fig. 5A, for the encapsulated protein it was possible to estimate the total number of protein molecules encapsulated within a single polymersome. This is possible due to the device output solution information previously being established from experimentation, which then enables the final sepharose filtered solution properties to be obtained. The calculated results enable accurate comparison of the encapsulation efficiency between the two different formation processes. The outcome of this calculation is presented in Fig. 5B where the device has 340 (±29%) BSA molecules encapsulated per polymersome and the standard solution method resulted in 311 (±27%). Both formation methods result in comparable numbers of encapsulated BSA molecules within the polymersome structures, and indicate that the encapsulation efficiency for the flow focussing device is analogous to the standard formation method. This makes it a viable alternative for encapsulating molecules within the hydrophilic core of polymersomes for cellular transport applications or as biomimetic nanoscale reaction containers.

There are a number of advantages that enhance the functionality of the microfluidic polymersome formation process. Firstly, the continuous production process means that one chip running with the 8 : 48 μl min^{-1} flow rate produces 1 ml of polymersomes in approximately 9 minutes. From the same starting point the standard method takes around 30 minutes and this is clearly a significant reduction in production time. This is mainly due to the removal of the sonication post-processing step. Due to the bulk nature of production, this time remains near constant for increasing volumes. However, due to the strength of the irreversible seal, the flow rates of the device can be increased at least 20 times, significantly amplifying the polymersome production rate. This rate can be further increased due to the ease at which this simple flow focussing PDMS device can be scaled up, with numerous devices running simultaneously off one set of inlets. Large quantities of polymersomes could be produced in a greatly reduced time to the current bulk production processes for the volumes required for the current applications. However, this time could be reduced still further if the length of the serpentine channel was adjusted, whereby this distance controls the dilution of the polymersomes. Varying the length of the serpentine channel across a series of parallel flow focussed channels would

provide the potential that a single device with one set of inlets would be able to continuously produce polymersomes over a range of predetermined concentrations. This could dramatically increase the speed at which studies to identify the correct dosage are carried out, as well as reducing the problems of batch to batch variation in polymersome samples. The uncomplicated process lends itself to a very quick and user friendly method for producing polymersomes with the desired hydrophilic encapsulate. The device can be effortlessly automated, and we believe is the first step towards a completely automatic system that enables polymersomes with the desired properties to be produced on demand within the laboratory. Work is in progress on providing control over the size distribution of the polymersomes *via* linking the microfluidic device to an extruder pump. In addition, the varying polymer concentration throughout the device may enhance the formation of polymersomes and increase their overall yield and research is ongoing to determine whether this is the case.

Conclusions

The results of this study demonstrate that a microfluidic system has been developed that enables the continuous production of biocompatible polymersomes, using the controlled diffusion of pH within the microchannels to induce stable self-assembly without the use of organic solvents. Analysis using DLS and TEM has demonstrated that the device produces polymersomes of the same size and polydispersity as standard production methods, with polymersome diameters generally within 75 nm to 275 nm. Additionally, calculations of the encapsulation efficiency indicate the device is comparable to the standard in solution production method of encapsulating hydrophilic molecules. Both these factors clearly indicate that the polymersomes produced are fit for the current intracellular delivery applications for drugs, DNA and proteins. The benefits of the continuous production process, with the dramatic reduction in production time, removal of bulk variation, potential accurate control over concentration, removal of organic solvents from the production process and the reproducibility of the system, give the device great potential for wider usage. The ease at which PDMS microfluidic devices can be scaled up gives the system the capability to be fully automated incorporating the current post-processing step of extrusion to narrow the size distribution for intracellular delivery. This could also include the filtration step to remove the un-encapsulated material by introducing a channel or additional device containing the sepharose beads, dramatically increasing the ease of the entire process.

In conclusion, we believe that the benefits associated with continuous polymersome production and the potential of the system to be fully automated demonstrate that flow focussing microfluidic devices offer a viable alternative production process for polymersomes for intracellular delivery applications.

Acknowledgements

The authors would like to thank the EPSRC (DTA award and grants GR/S84347/01 and EP/E036252/1) for funding this research and special thanks goes to Mr Simon Forster for his work in setting up the department's equipment to produce microfluidic devices. Thanks are also due to Prof. Steven Armes and Biocompatibles Ltd. for polymer production, Dr Caterina Lo Presti for producing the TEM images and Denis Cecchin for his guidance in protein encapsulation.

References

1 C. Hansen and S. R. Quake, *Curr. Opin. Struct. Biol.*, 2003, **13**, 538–544.
2 S. Y. Teh, R. Lin, L. H. Hung and A. P. Lee, *Lab Chip*, 2008, **8**, 198–220.
3 T. M. Squires and S. R. Quake, *Rev. Mod. Phys.*, 2005, **77**, 977–1026.
4 T. Thorsen, R. W. Roberts, F. H. Arnold and S. R. Quake, *Phys. Rev. Lett.*, 2001, **86**, 4163–4166.
5 G. F. Christopher and S. L. Anna, *J. Phys. D: Appl. Phys.*, 2007, **40**, R319–R336.
6 W. Jeong, J. Kim, S. Kim, S. Lee, G. Mensing and D. J. Beebe, *Lab Chip*, 2004, **4**, 576–580.
7 S. L. Anna, N. Bontoux and H. A. Stone, *Appl. Phys. Lett.*, 2003, **82**, 364–366.
8 A. Jahn, J. E. Reiner, W. N. Vreeland, D. L. DeVoe, L. E. Locascio and M. Gaitan, *J. Nanopart. Res.*, 2008, **10**, 925–934.
9 R. K. Shah, H. C. Shum, A. C. Rowat, D. Lee, J. J. Agresti, A. S. Utada, L. Y. Chu, J. W. Kim, A. Fernandez-Nieves, C. J. Martinez and D. A. Weitz, *Mater. Today (Oxford, UK)*, 2008, **11**, 18–27.
10 A. Jahn, W. N. Vreeland, D. L. Devoe, L. E. Locascio and M. Gaitan, *Langmuir*, 2007, **23**, 6289–6293.
11 A. Jahn, W. N. Vreeland, M. Gaitan and L. E. Locascio, *J. Am. Chem. Soc.*, 2004, **126**, 2674–2675.
12 H. Lomas, I. Canton, S. MacNeil, J. Du, S. P. Armes, A. J. Ryan, A. L. Lewis and G. Battaglia, *Adv. Mater.*, 2007, **19**, 4238–4243.
13 D. E. Discher, V. Ortiz, G. Srinivas, M. L. Klein, Y. Kim, C. A. David, S. S. Cai, P. Photos and F. Ahmed, *Prog. Polym. Sci.*, 2007, **32**, 838–857.
14 P. P. Ghoroghchian, P. R. Frail, K. Susumu, D. Blessington, A. K. Brannan, F. S. Bates, B. Chance, D. A. Hammer and M. J. Therien, *Proc. Natl. Acad. Sci. U. S. A.*, 2005, **102**, 2922–2927.
15 S. Z. Razzacki, P. K. Thwar, M. Yang, V. M. Ugaz and M. A. Burns, *Adv. Drug Delivery Rev.*, 2004, **56**, 185–198.
16 J. K. Oh, R. Drumright, D. J. Siegwart and K. Matyjaszewski, *Prog. Polym. Sci.*, 2008, **33**, 448–477.
17 S. Sugiura, T. Oda, Y. Izumida, Y. Aoyagi, M. Satake, A. Ochiai, N. Ohkohchi and M. Nakajima, *Biomaterials*, 2005, **26**, 3327–3331.
18 E. Lorenceau, A. S. Utada, D. R. Link, G. Cristobal, M. Joanicot and D. A. Weitz, *Langmuir*, 2005, **21**, 9183–9186.
19 R. C. Hayward, A. S. Utada, N. Dan and D. A. Weitz, *Langmuir*, 2006, **22**, 4457–4461.
20 H. J. Oh, S. H. Kim, J. Y. Baek, G. H. Seong and S. H. Lee, *J. Micromech. Microeng.*, 2006, **16**, 285–291.
21 A. Taubert, *Proc. Natl. Acad. Sci. U. S. A.*, 2007, **104**, 20643–20644.
22 M. J. Doktycz and M. L. Simpson, *Mol. Syst. Biol.*, 2007, **3**, 1–10.
23 D. E. Discher and A. Eisenberg, *Science*, 2002, **297**, 967–973.
24 G. Battaglia and A. J. Ryan, *Nat. Mater.*, 2005, **4**, 869–876.
25 G. Battaglia and A. J. Ryan, *J. Phys. Chem. B*, 2006, **110**, 10272–10279.
26 B. M. Discher, Y. Y. Won, D. S. Ege, J. C. M. Lee, F. S. Bates, D. E. Discher and D. A. Hammer, *Science*, 1999, **284**, 1143–1146.
27 J. Z. Du, Y. P. Tang, A. L. Lewis and S. P. Armes, *J. Am. Chem. Soc.*, 2005, **127**, 17982–17983.
28 H. Lomas, M. Massignani, K. A. Abdullah, I. Canton, C. Lo Presti, S. MacNeil, J. Z. Du, A. Blanazs, J. Madsen, S. P. Armes, A. L. Lewis and G. Battaglia, *Faraday Discuss.*, 2008, **139**, 143–159.
29 M. Massignani, C. LoPresti, A. Blanazs, J. Madsen, S. P. Armes, A. L. Lewis and G. Battaglia, *Small*, 2009, **5**, 2424–2432.
30 C. LoPresti, H. Lomas, M. Massignani, T. Smart and G. Battaglia, *J. Mater. Chem.*, 2009, **19**, 3576–3590.
31 G. Battaglia and A. J. Ryan, *J. Am. Chem. Soc.*, 2005, **127**, 8757–8764.
32 G. Battaglia, A. J. Ryan and S. Tomas, *Langmuir*, 2006, **22**, 4910–4913.
33 A. S. Utada, E. Lorenceau, D. R. Link, P. D. Kaplan, H. A. Stone and D. A. Weitz, *Science*, 2005, **308**, 537–541.

34 H. C. Shum, J. W. Kim and D. A. Weitz, *J. Am. Chem. Soc.*, 2008, **130**, 9543–9549.
35 M. K. Chaudhury and G. M. Whitesides, *Langmuir*, 1991, **7**, 1013–1025.
36 D. C. Duffy, J. C. McDonald, O. J. A. Schueller and G. M. Whitesides, *Anal. Chem.*, 1998, **70**, 4974–4984.
37 C. S. Effenhauser, G. J. M. Bruin, A. Paulus and M. Ehrat, *Anal. Chem.*, 1997, **69**, 3451–3457.
38 V. Hearnden, H. Lomas, S. MacNeil, M. Thornhill, C. Murdoch, A. Lewis, J. Madsen, A. Blanazs, S. Armes and G. Battaglia, *Pharm. Res.*, 2009, **26**, 1718–1728.
39 L. Shen, J. Z. Du, S. P. Armes and S. Y. Liu, *Langmuir*, 2008, **24**, 10019–10025.
40 J. R. Howse, R. A. L. Jones, G. Battaglia, R. E. Ducker, G. J. Leggett and A. J. Ryan, *Nat. Mater.*, 2009, **8**, 507–511.

